RSC Advances

ROYAL SOCIETY OF CHEMISTRY

www.rsc.org/advances

RSC Advances

RSCPublishing

ARTICLE

Nanostructured Films by the Self-Assembly of Bioactive Copolymer

Cite this: DOI: 10.1039/x0xx00000x

O.V. Sinitsyna,[a] N.K. Davydova,*[a] V.N. Sergeev[a] and E.E. Laukhina*[b]

Received 00th October 2014,
Accepted 00th October 2014

DOI: 10.1039/x0xx00000x

www.rsc.org/

Synthesis of multifunctional macromolecules has become an important topic as advances are made in biological sensing technology. Various templates that may be quantified with presentation of bioactive molecules and control over their density and orientation are required. The paper shows that thin films based on a bioactive copolymer acrylamide/N-(2-dibenzylamino-ethyl)-acrylamide (**1**) with arrays of submicro- and nanoscale cavities can be formed at ambient conditions using a self-organization method such as a dewetting process. We showed that the concentration of **1** in its water solution as well as the hydrophobicity of a film support are key parameters allowing to control over a nanocavities formation on the surfaces of thin films of **1**; the surface morphologies were studied using Atomic Force Microscopy (AFM). The simple procedure used for engineering DNA trapping nanocavities on the surface of the bioactive thin films of **1** makes these films very promising for applications where nanoscale detection of biomacromolecules is required.

Introduction

Bioactive nanostructured surfaces are of strong interest with respect to basic research as well as for future biomedical applications. For example, progress has been done in transplantation of "encapsulate" beta cells using both natural and synthetic membranes. Such membranes have pores being large enough to allow insulin and glucose to pass freely, but these pores are small enough to permit antibodies to reach and target the transplanted foreign beta cells.[1,2] On the other hand, nanopores of specific characteristics are very useful for the successful detection of biomolecule complexes.[3-6] O. A. Saleh and L. L. Sohn successfully demonstrated the capabilities of the nanopores-based device to sense electronically single DNA molecules.[7] Porous nanocapsules and polymer hydrogels are extremely interesting for cell and drug delivery.[8-11] In this context, the development of thin films based on multifunctional macromolecules that are able to recognize different biomacromolecules has become an important topic. Recently, we described the synthesis of the copolymer acrylamide/N-(2-dibenzylamino-ethyl)-acrylamide (**1**, Fig. 1a, b) and showed that **1** uniting with double-stranded DNA is able to form a set of various nanostructures.[12,13]

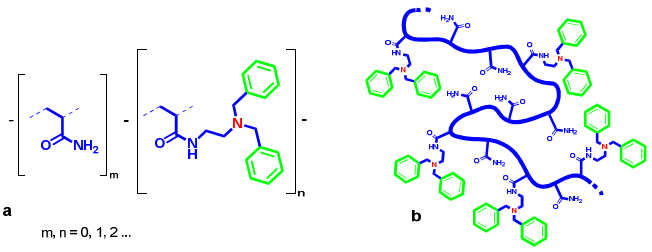

Fig. 1 Skeletal formula (**a**) and schematic image (**b**) of copolymer **1.**

Most likely the electrostatic trap of DNA molecules by bioactive copolymer **1** results in the formation of nanostructures reported by some of the authors of this article.[12]

To extend the capability of **1** to be used as a biomacromolecules sensing component, the preparation of thin **1**-based films with controlled nanocavities surfaces have to be developed. Engineering such sensing films is related to nanotechnology that is of great importance for industry striving for novel miniature sensing devices. Taking into account that dewetting of polymeric films may be successfully used for engineering nanostructured polymer surfaces,[14] we used it for building-up nanostructured **1**-based films that was a goal of this paper. AFM was applied for the nano-scale study of the surfaces of developed films.

Here we present the preparation of nano-patterns of thin **1**-based films using a dewetting process. The effect of the concentration of **1** in its water solution on the nanopattern of the film surfaces is demonstrated. We also describe the important role of the hydrophobicity of a supporting substrate in **1**-based film stability.

Experimental

Copolymer synthesis. **1** was prepared by free-radical polymerization in aqueous medium using red-ox system of ammonium persulfate – tetramethyl-ethylenediamine as it was reported.[12]

Supports preparation. Natural mica crystals and highly oriented pyrolytic graphite (HOPG) were chosen as hydrophilic and hydrophobic supports, respectively. They were cleaved just before the experiments using Scotch tape. HOPG was produced by Atomgraph-crystal.

Films preparation: The water solutions of different concentrations of **1** (3 mg/ml, 0.03 mg/ml, and ≅0.003 mg/ml) were prepared using bidistilled water; films were cast from the water solutions of **1** over mica- and graphite-based supports (2.5 µl) and dried under ambient conditions. The names of the films and their characteristics are summarized in Table 1. For comparative purpose, two films of each type were prepared.

DNA trapping experiment. 0.01 mg/ml water solution of λ-phage DNA (Fermentas) was used in DNA trapping experiments. Drops of the DNA solution (1 µl) were applied to the surfaces of films B. Then the samples were dried at ambient conditions.

Surface morphology analysis. The textures of **1**-based films were investigated using multifunctional scanning probe microscope "FemtoScan", produced by Advanced Technologies Center. Scanning was performed in contact and tapping modes of AFM; fpC11 cantilevers, produced by Institute of Physical Problems named after F.V. Lukin, were used in the contact mode and MikroMasch cantilevers of the 15 series were used in the tapping mode. The experimental AFM data were processed and analyzed by the "FemtoScan Online" software (Advanced Technologies Center).

Measurements of the films thickness. The thickness of film A was estimated by micrometer "MK25" (Kalibr). The thickness of films B, C, and D was measured by AFM. The copolymer was removed in a small area by AFM tip in contact mode, and then the area was imaged in tapping mode to determine the height difference between the copolymer and the substrate surfaces (Fig. S1, ESI).

Results and discussion

To generate a patterned surface of **1**-based film at the nanometric level, we used a dewetting process. Assuming that viscosity of casting solutions might be one of the key parameters, which determines a film formation process, the surface properties of **1**-based films were tailored by controlling the initial concentration of **1** in its water solutions. In line with research aim we prepared **1**-based films (A, B, and C) over the surface of a mica crystal from solutions that significantly differ in concentration (see Table 1). The fourth sample, film D, was formed over a graphite surface from the same water solution that was used for film B casting; all films were prepared by drop casting method at ambient conditions. Morphologies of the surfaces of the developed films were studied using AFM. It is necessary to note that it was not possible to observe any difference between the surface morphologies of initial films A, B, C, D and the textures of their duplicates. Table 1 indicates the manner in which the morphology of **1**-based film varies with casting conditions.

Table 1 The effect of concentration (C) of **1** and the nature of supporting substrates on surface morphologies of the bioactive **1**-based films.

Film type	C mg/ml	Supporting substrate	Cavities morphology		Cavities density
			Diameter, nm	Depth, nm	Cavities/µm^2
A	3.00	mica crystal	218±71	1.9±1.2	10/100
B	0.03	mica crystal	300±230	9.4±3.7	150-160/100
C	≅0.003	mica crystal	51±16	1.5±0.2	4500/100
D	0.03	graphite	111±80	13±10	100-150/100

Surface morphology of film A prepared from a concentrated water solution

The AFM image of film A (Fig. 2a, b) shows a smooth surface with some very shallow cavities being few in number: 10 cavities per 100 µm^2. The average cavity diameter is 218±71 nm and the average cavity depth is really very small: it was found as 1.9±1.2 nm. The maximum height difference was found as 30 nm in defect-free areas with the square of 4 µm^2, the root-mean-square roughness being 0.8 nm. Therefore, at the concentration of **1** being 3 mg/ml, the viscosity of its initial water solution is enough to yield films, being stable to a hole formation. In this case one may conclude that film A is thick enough to prevent the hole formation process which is conducted by the surface tension force: there is a lot of film's mass to transfer to enable hole growth. The thickness of film A was (10±5) µm.

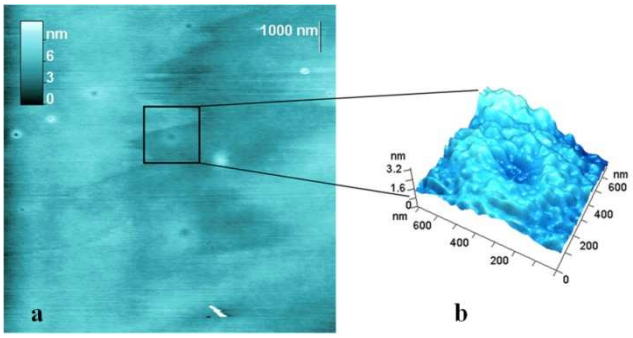

Fig. 2 The typical AFM image of the surface of film A cast over a mica crystal; the frame size is 10.3x10.3 µm^2 (**a**), and 3D AFM image of one of the cavities (**b**).

Morphology of film B prepared from a diluted water solution

In contrast to film A, the surface of film B has a regular nanostructure, which is shown in Fig.3a, b, and Fig. S2, ESI. The average cavity diameter is 300 nm (the standard deviation of 230 nm). The average cavity depth is about ten nanometers (Table 1). The data were calculated for 60 cavities. The film was partially removed from the mica surface by AFM tip in contact mode that allowed us to measure the film thickness, which was about 10 nm.

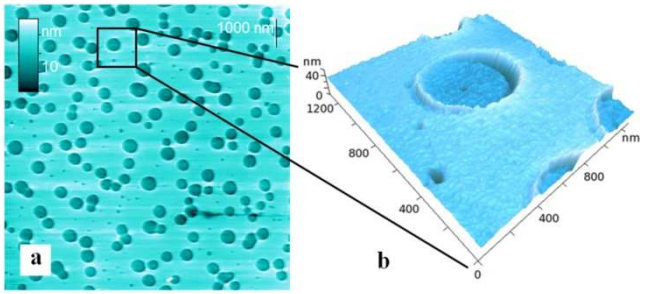

Fig. 3 The typical AFM image of the surface of film B over a mica crystal (the frame size is 10.1x10.1 µm^2, **a**), and 3D AFM image of one of the cavities (**b**).

Some wide cavities, which have the diameters from 1000 nm to 2500 nm and the depth of 11.8-11.9 nm, may be also observed (Fig. S2, ESI). Below we will focus on some details of hole morphologies (Fig. 3). To compare properly textures inside and outside the cavities the filter "highlight" was applied to the AFM image of the surface of film B (Fig. 4).

As may be seen from Fig. 4 it is not possible to find any difference between the surface structure inside and outside the cavity. But the root-mean-square roughness was slightly higher for the inner region. The roughness was calculated for the regions with the area of 0.11 µm^2. The roughness parameters are listed in Table S1, ESI.

Since the mica surface is atomically smooth, its roughness is determined mainly by the noise of the microscope. The noise level doesn't exceed 0.1 nm. As the surface roughness inside the pores is an order of magnitude larger than the roughness of pure mica, one may suggest that a very thin wetting layer of **1** remains on the mica surface.

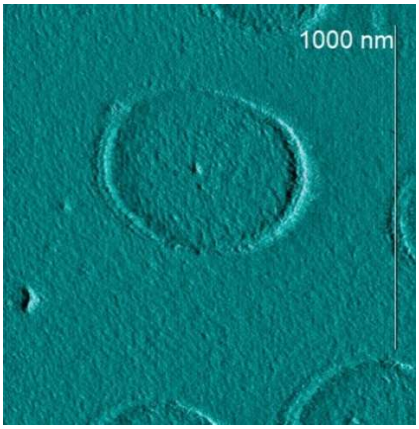

Fig. 4 AFM image of the cavity formed on the surface of film B cast over a mica crystal. The frame size is 1.24x1.24 μm^2; the filter "highlight" was applied to the image.

The stability of a thin film is governed by the dependence of the effective interface potential on the film thickness.[15] The presence of the wetting layer on the mica surface indicates the existence of a global minimum of the effective interface potential at critical thickness equal to the thickness of the layer inside the cavity. The root-mean-square roughness of the wetting layer of 1.7 nm may be considered as a lower-bound estimation for the critical thickness.

The lateral forces distribution (Fig. S3 b) shows that the areas inside the large cavities are characterized by a higher value of the lateral forces. One of the possible reasons of the high lateral forces may be the increase of the surface roughness inside the cavities. Moreover, mica becomes negatively charged in water solutions. The smaller the thickness of the copolymer film, the weaker it screens the charge. The additional electrostatic interaction between the AFM probe and the surface also can lead to the stronger lateral forces.

Below we will clarify some details of hole growth in very thin film B (h~10 nm). It is known that thin films are unstable to hole formation.[16] As the high regularity of cavities is observed in the AFM image of film B (Fig. 3a), nucleation of holes is initiated by a spontaneous (spinodal) process rather than by the process of hole nucleation at some defects. In this case dispersion forces are at play that results in the unstable form of a thin film with a very high surface-to-volume ratio which in turn causes the hole to grow.[16] Here it is pertinent to mention that **1** contains N-(2-dibenzylamino-ethyl)-acrylamide which has hydrophobic benzyl moieties. Schematically cavities formation may be presented as it is shown in Fig.S4, ESI.

After water evaporation, the mobility of macromolecules of **1** becomes significantly smaller, which prevents further changes in the morphology of the film. The film demonstrated good long-term stability: the AFM studies did not able to reveal any alterations of its morphology during storage at ambient conditions (see Fig.S5, ESI). Additionally it should be noted that **1** also retained its bioactivity manifested in the capability to form filamentous complexes with DNA (see Fig.S6 a, b, ESI).

Trapping DNA by nanostructured film B

To clarify the ability of nano-cavities formed at the surface of film B to trap DNA molecules we dripped of a drop of a DNA water solution on the surface of film B. As Fig. 5a, b shows, convex particles with the height of about 5.8±1.5 nm are clearly visible instead of the cavities. The particles diameter (318±39) and their surface density (150/100 μm^2) are just the same as for the cavities. Maps of lateral forces distribution were obtained simultaneously with topographic images (see Fig.S7a, b, ESI). Their analysis revealed a decrease of lateral forces in areas of the particles location. Thus the trapped particles demonstrate different nanotribological response comparison with those of **1**-based film.

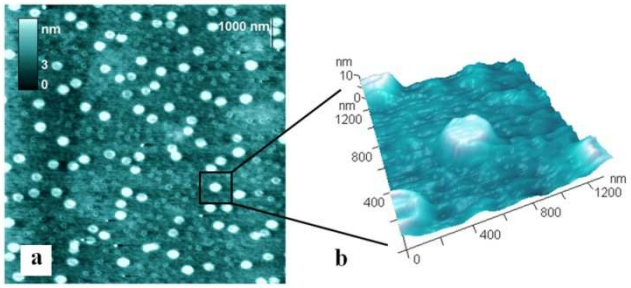

Fig. 5 The typical AFM image of the surface of film B over a mica crystal with trapped DNA molecules (the frame size is 10.1x10.1 μm^2, **a**), and 3D AFM image of one of the particles (**b**).

The observed changes of both film morphology and lateral forces distribution may be explained in terms of electrostatic trapping of DNA molecules by the film cavities. The film-forming molecules of **1** contain tertiary amine groups that are usually protonated in water solutions.[17] Thus, the surface of **1**-based film is positively charged when a DNA water solution comes into contact with it. On the other hand, DNA molecules are negatively charged in DNA water solutions.[18] Therefore, in the present of water molecules the positive charged surface of **1**-based film is able to trap negative charged DNA molecules using electrostatic interactions. The cavities are the most preferable sites for DNA binding because their surface geometry is able to provide a greatest number of electrostatic interactions (Fig. 6). By our assumption, the water evaporation may lead to the formation of compact DNA-based particles being mainly located at the film cavities.

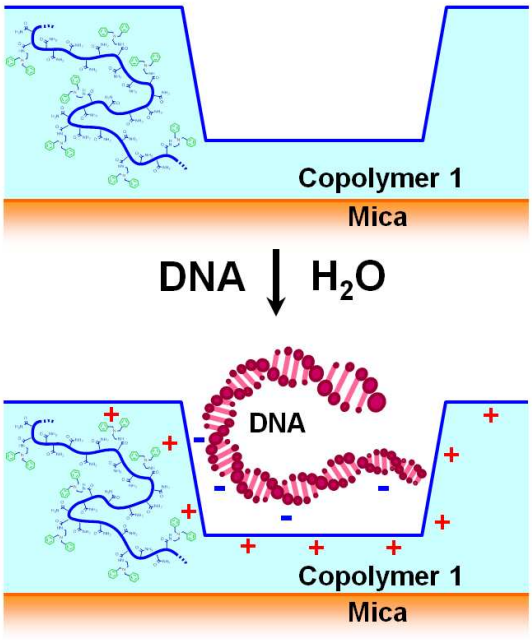

Fig. 6 Scheme of DNA trapping by the cavities of film B.

Surface morphology of film C prepared from the most diluted solution

To further decrease films thickness and increase the surface-to-volume ratio, **1** was deposited from the most diluted solution (≅0.003 mg/ml) over a mica crystal (film C). Its AFM investigation revealed the formation of cavities with average diameter of about 50 nm (Fig 7 a, b). Details of the cavities morphology are listed in Table 1. Their shape deviates significantly from the form of a circle. By our assumption, this effect is related to the partial coalescence of the cavities. Interesting to note that their surface density is significantly higher for film C in comparison with that for film B, which indicates a strong increase in the amount of cavities nucleation centers in the thinner film. The thickness of film C is about 1.5 nm.

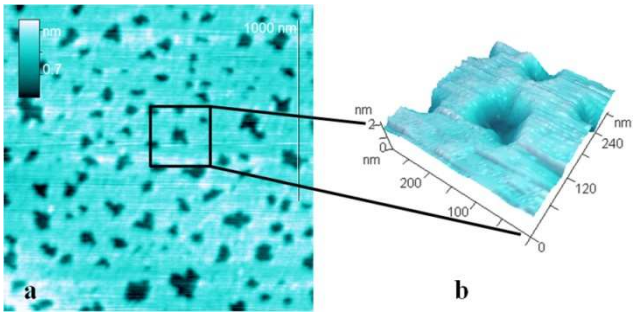

Fig. 7 The typical AFM image of the surface of film C cast over mica (the frame size is 1.5x1.5 μm^2, **a**) and 3D AFM image of one of the cavities (**b**).

Our attempts to prepare a film over the mica surface from more diluted solutions of **1** resulted in its self-assembling as separated "islands" (see S8, ESI).

As a mica surface is hydrophilic,[19, 20] hydrophobic components of **1** might significantly reduce stability of the film due to increasing the interface potential between it and mica surface. If this is the case, there are bound to be substrates which, thanks to their hydrophobic properties, will be able to decrease the interface potential between **1**-based film and a substrate surface that in turn may stabilize the thin **1**-based films.

Surface morphology of film D cast over a hydrophobic support

To clarify this additional ability to control over nanostructured surfaces of bioactive **1**-based films we prepared film D over a graphite surface from the same water solution that was used for film B casting.

Film D on the graphite surface (Fig. 8a, b) has also cavities, but the mean pore diameter is 111 nm (standard deviation of the average diameter is 80 nm), which is three times smaller than in the case of the mica substrate (film B, Fig. 3). Moreover, as Fig.8 shows, the cavity density is slightly less in comparison with that observed for the film prepared over a hydrophilic mica surface.

There is a difference between the values of the pore depth in the trace and the retrace (forward and backward direction) for a line in the AFM images of film D. According to our assumption, the effect is caused by the twist motion of the cantilever beam as it passes the surface regions with sharp changes in topography. Taking into account the twist motion of the cantilever beam, the pore depth is calculated as half the sum of the pore depths measured in the trace and the retrace images. Depth averaged over all found pores is 13 nm; the standard deviation of the depth is 10 nm.

Cavities in the film were created for additional control of the film thickness. For this purpose, preliminary scan was carried out in a resonant mode. Then a small area was selected and scanned in a contact mode with a large force (~ 50 nN). As a result, upper surface layers were destroyed and a cavity was formed. The surface structure of graphite was preserved inside a cavity with the depth of ~ 8 nm, whereas the graphite structure was changed inside a cavity with the depth of ~ 20 nm that indicated the damage of the substrate. Thus, we concluded that the film thickness of the copolymer lies in the range from 8 nm to 20 nm. The thickness of film B lies in the same range.

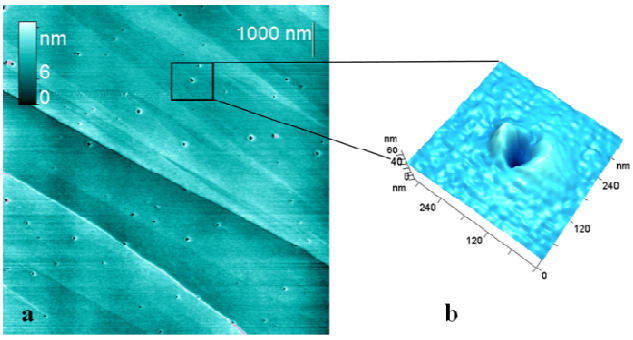

Fig. 8 The typical AFM images of the surface of film D over graphite (the frame size is 11.1x11.1 μm^2, **a**) and 3D AFM image of one of the cavities (**b**).

Cleavage steps were not observed in the images of **1**-based film, which was cast from a solution with a higher copolymer concentration, indicating the large thickness of the copolymer film. Cleavage steps with the height of 1 nm are visible for a **1**-based film, prepared from a solution with concentration of 0.03 mg/ml.

Conclusions

Our study shows that a dewetting process can be successfully utilized as a simple procedure for nano-scale engineering surface morphologies of bioactive films in which the copolymer acrylamide/N-(2-dibenzylamino-ethyl)-acrylamide is at play.

The protocol of the film casting, which permits one to reproducibly prepare **1**-based films with various regular cavity-like nanostructured surfaces, was developed.

The proof-of-concept experiments demonstrate the possibility of DNA trapping by nano-cavities formed at the surface of **1**-based films.

Thus the control over the morphology of **1**-based films paves the way for their use in biotechnological applications. On the other hand the sensitivity of **1** to biomacromolecules makes it a useful system for fundamental studies.

Acknowledgements

1. The work was supported by the Agreement with Ministry of Education and Science of Russian Federation.

2. E.L. thanks CIBER-BBN, an initiative funded by the VI National R&D&i Plan 2008-2011, Iniciativa Ingenio 2010, Consolider Program, CIBER Actions and financed by the Instituto de Salud Carlos III with assistance from the European Regional Development Fund.

Notes

[a] A.N. Nesmeyanov Institute of Organoelement Compounds of Russian Academy of Sciences, Moscow, Russian Federation.
[b] The Biomedical Research Networking center in Bioengineering, Biomaterials and Nanomedicine, ICMAB-CSIC, Bellaterra, 08193, Spain

*E-mails: davydova@ineos.ac.ru and laukhina@icmab.es

† Electronic Supplementary Information (ESI) available: [Roughness parameters for surfaces inside and outside the typical cavity. Film B thickness measurement. Typical AFM image of the surface of film B cast over a mica crystal showing large cavities. The images of topography and lateral force distribution on film B. Scheme of the cavities formation in film B. Typical AFM image of the surface of film B stored six months at ambient conditions. Typical AFM image of the complex between λ-DNA and copolymer **1** formed on the mica surface (the sample of copolymer **1** was synthesized six month before the DNA trapping experiment) and schematic view of the complex formation. The images of topography and lateral force distribution on film B with trapped DNA molecules. Typical AFM image of "islands" which are formed on a mica crystal from very diluted water solution of copolymer 1]. See DOI: 10.1039/b000000x/

References

1 http://www.diabetesnet.com/beta-cell-transplants
2 G. Orive, R.M. Hernández, A.R. Gascón, R. Calafiore, T.M.S. Chang, Paul de Vos, G. Hortelano, D. Hunkeler, I. Lacík, A.M.J. Shapiro, J.L. Pedraz, *Nature Medicine,* 2003, **9** (1), 104-107.
3 S. Howorka, Z. Siwy, *Chem. Soc. Rev.*, 2009, **38** (8), 2360–2384.
4 J. Shim, G.I. Humphreys, B.M. Venkatesan, J.M. Munz, X. Zou, C. Sathe, K. Schulten, F. Kosari, A.M. Nardulli, G. Vasmatzis, R. Bashir, *Sci. Rep.*, 2013, **3**, 1389.
5 R.M.M. Smeets, S.W. Kowalczyk, A.R. Hall, N.H. Dekker, C. Dekker, *Nano Lett.*, 2009, **9**, 3089–3095.
6 J. Shim, J.A. Rivera, R. Bashir, *Nanoscale*, 2013, **5**, 10887–10893.
7 O.A. Saleh, L.L. Sohn, *Nano Lett.*, 2003, **3**(1), 37-38.
8 P. Petrov, E. Petrova, C.B. Tsvetanov, *Polymer,* 2009, **50**, 1118-1123.
9 P. Petrov, D. Momekova, B. Kostova, G. Momekov, N. Toncheva-Moncheva, C.B. Tsvetanov, N. Lambov, *J. Control. Release*, 2010, **148**, e74–e84.
10 P. Petrov, C.B. Tsvetanov, *Polymeric Cryogels: Macroporous Gels with Remarcable Properties, Series: Advances in Polymer Science*, 2014, **263**, 199-222.
11 B. Daglar, E. Ozgur, M.E. Corman, L. Uzun, G.B. Demirel, *RSC Adv.*, 01 Sep 2014, DOI: 10.1039/C4RA06406B.
12 N.K. Davydova, O.V. Sinitsyna, I.V. Yaminsky, E.V. Kalinina, K.E. Zinoviev, *Macromolecular Symposia,* 2012, **321-322** (1), 84 -89.
13 N.K. Davydova, O.V. Sinitsyna, K.E. Zinoviev, *AIP Conf. Proc.*, 2012, **1459**, 220-222.
14 P. Müller-Buschbaum, *J.Phys.:Condens.Matter,* 2003, **15**, R1549.
15 O. Bäumchen, K. Jacobs, *J. Phys.: Condens. Matter,* 2010, **22**, 033102.
16 K. Dalnoki-Veress, J.R. Dutcher, J.A. Forrest, *Physics in Canada*, 2003, **59**(2), 75-84.
17 M. B. Smith, J. March, *March's Advanced Organic Chemistry: Reactions, Mechanisms, and Structure,* Wiley, New Jersey, 6th edn., 2007.
18 M. J. Tiera, Q. Shi, F. M. Winnik, J. C. Fernandes, *Curr. Gene Ther.*, 2011, Aug, **11**(4), 288-306.
19 D.H. Bangham, Z. Saweris, *Trans. Faraday Soc*., 1938, **34**, 554-570.
20 J. Drelich, E. Chibowski, D.D. Meng, K. Terpilowski, *Soft Matter,* 2011, **7**, 9804-9828.

Nanostructured Film by the Self-Assembly of Bioactive Copolymer

O.V. Sinitsyna, N.K. Davydova,* V.N. Sergeev and E.E. Laukhina*

We have developed a route via a simple dewetting process that permits one to control over the cavities formation on the surfaces of thin films based on bioactive copolymer which is able to trap DNA.

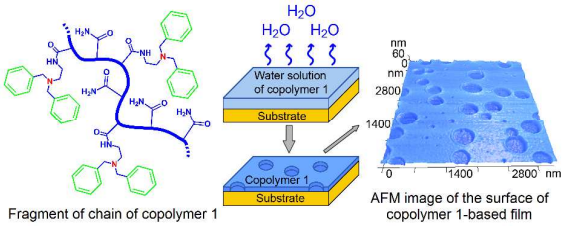

Fragment of chain of copolymer 1

AFM image of the surface of copolymer 1-based film